

On The Robustness of Asthenosphere Plug Flow in Mantle Convection Models With Plate-Like Behavior

Adrian Lenardic¹ and Alana Semple¹

¹Rice University

November 21, 2022

Abstract

The question of what drives tectonic plates has been revitalized by seismic observations that cannot be explained by conventional plate-driving forces. The observations, designed to constrain flow in the asthenosphere, are consistent with the asthenosphere locally flowing faster than the plate above and in a direction offset from plate motion. These inferences are not consistent with plates being driven exclusively by slab-pull and/or ridge-push forces. Mantle convection models were put forth to argue that pressure-driven flow, interacting with a non-Newtonian upper mantle viscosity, could explain these observations. To test the robustness of those results, we expand the models to allow for the development of weak plate margins and associated plate-like behavior. We find that with weak margins, the overall component of slab-driven flow becomes stronger while pressure driven asthenosphere flow remains active. Locally, the asthenosphere can lead plates and there are rotations in the direction of asthenosphere flow with depth. The balance of plate driving forces (i.e., the ratio of slab-pull to asthenosphere flow) is found to depend on plate margin strength. The models also indicate that a non-Newtonian upper mantle allows for a hysteresis effect such that, depending on initial conditions, single-plate and plate-tectonic modes can exist at the same parameter conditions.

1 **On The Robustness of Asthenosphere Plug Flow in**
2 **Mantle Convection Models With Plate-Like Behavior**

3 **Alana Semple¹, Adrian Lenardic¹**

4 ¹Rice University

5 **Key Points:**

- 6 • Weak plate margins and a power law viscosity asthenosphere allow asthenosphere
7 flow to exceed lithosphere velocity
8 • There are local regions where asthenosphere flow rotates with depth away from
9 lithosphere flow direction
10 • Mobile vs stagnant lid state depends on lid strength and initial condition when
11 the asthenosphere has a power law viscosity

Corresponding author: Alana Semple, ags7@rice.edu

Abstract

The conventional hypothesis holds that tectonic plates are driven exclusively by slab-pull/ridge-push forces, but this is challenged by recent seismic observations of asthenosphere flow. These observations indicate that the asthenosphere locally flows faster and in a different direction than the plate above. Previous mantle convection models argued that pressure-driven flow with a non-Newtonian upper mantle viscosity can account for these observations. We expand those models by simulating simple plate breaking behavior in plate margins. Under these conditions, the ratio of slab-driven flow to pressure-driven asthenosphere flow increases while pressure driven flow remains active. The ratio of driving forces decreases with increasing plate margin strength. Locally, the asthenosphere can drive plates and change flow direction with depth. Furthermore, a non-Newtonian upper mantle allows for a hysteresis effect where, depending on initial conditions, single-plate (stagnant lid) and plate-tectonic modes can exist at the same parameter conditions.

Plain Language Summary

Conventional wisdom holds that the motion of tectonic plates drives motion in the Earth's rocky interior (i.e., in the Earth's asthenosphere). Recent seismological observations have brought this view into question as they indicate that the velocity of the asthenosphere can exceed tectonic plate velocity. This suggests that interior motions can drive plate motions. We explore models of coupled plate tectonics and interior motions to address this discrepancy. The models reveal that the coupling between plates and the asthenosphere is not an issue of plates drive asthenosphere motion or asthenosphere motion drives plates. Both factors work in tandem with the balance being a function of plate margins strength and asthenosphere rheology. In particular, a power-law viscosity allows pressure gradients to generate interior flow that can locally drive plate motion. The models also reveal a hysteresis effect that allows different tectonic states (plate tectonics versus a single plate planet) to exist at the same parameter conditions. This indicates that history and initial conditions can play a role in determining if a planet will or will not have plate tectonics.

1 Introduction

Since the early days of the plate tectonic revolution, the leading idea for what drives plates has been slab-pull (Cox, 1972; Forsyth & Uyeda, 1975; Schubert et al., 2001; Turcotte & Schubert, 2014). More recent studies have questioned this and argued for a combination of slab-pull and pressure driven asthenosphere flow (Höink et al., 2011; Coltice et al., 2019). Seismic observations from the central Pacific added support to this idea as they could not be accounted for by invoking purely slab-driven flow (Lin et al., 2016). A subsequent study showed that the results were consistent with pressure driven flow interacting with a non-Newtonian upper mantle (Semple & Lendaric, 2018).

The study of Semple and Lendaric (2018) was motivated by seismic observations that showed two distinct shear zones in the asthenosphere and a mis-orientation between asthenosphere and plate flow directions (Lin et al., 2016). The models of Semple and Lendaric (2018) included a power law, upper mantle rheology within a spherical mantle convection model. The power law rheology lead to the formation of a low viscosity channel below a higher viscosity plate analog (i.e., an asthenosphere formed dynamically). Pressure gradients developed in response to upper boundary layer thickening away from zones of upflow (Höink et al., 2011). The low viscosity of the asthenosphere layer allowed it to flow faster than the plate above, in response to the pressure gradient. The pressure driven flow profile flattened toward a plug shape due to the power law rheology. This produced two concentrated shear layers within the asthenosphere (Fig. 1). Spherical geometry allowed pressure gradients to become offset in direction from the direction of up-

61 per boundary layer flow generating a change in flow direction with depth (Fig. 1). These
 62 findings provided a physical interpretation for the observations of Lin et al. (2016).

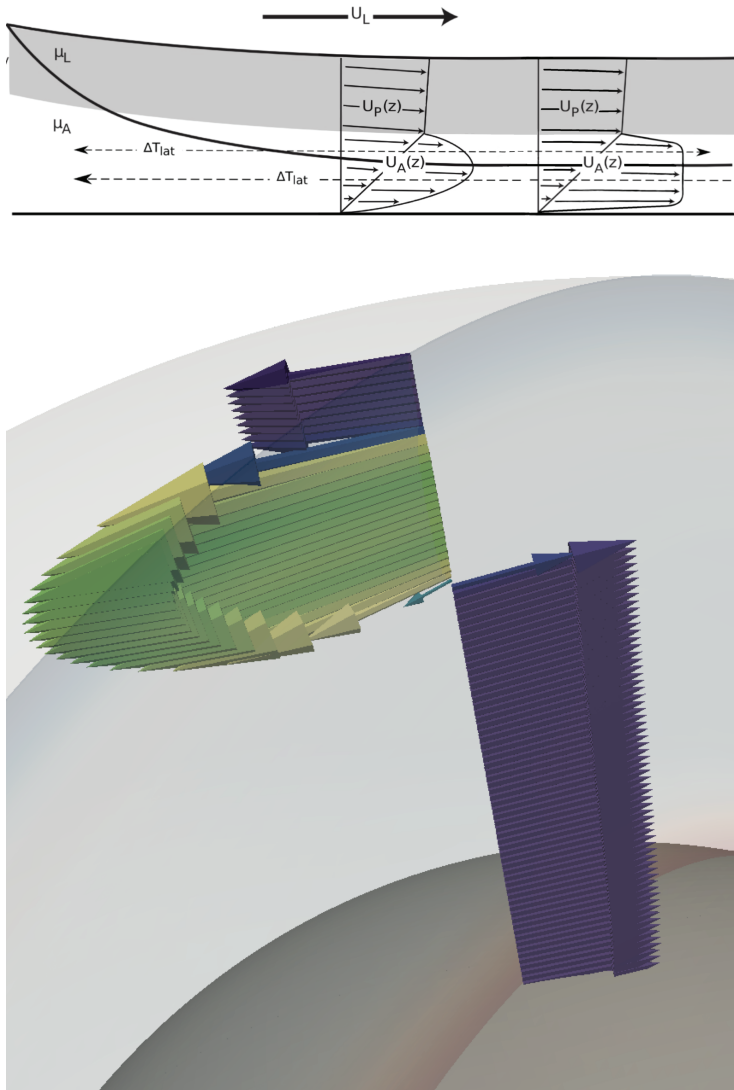


Figure 1. From Semple and Lenardic 2018. Top: Plug flow in the asthenosphere can develop where pressure gradients are strong and non-Newtonian viscosity is applied. Bottom: Newly plotted results from Semple and Lendardic (2018). Perspective view of a velocity profile for their $n=3$ results. Arrows are velocity vectors colored by viscosity where purple is 1 and greens are very low viscosity. This shows a location with plug flow in the asthenosphere and asthenosphere flow offset from lithosphere direction.

63 The study of Semple and Lendardic (2018) did not include weak plate margins. Flow
 64 in the models was partially driven by the sinking of cold upper boundary layer material
 65 into the mantle. This served as an analog for slab driven flow, but it is lacking in the
 66 sense that it may underestimate the strength of slab pull. Without weak plate margins,
 67 the high viscosity of a plate analog provides resistance to mantle downflow. Allowing for
 68 weak plate margins would alter this resistance and could enhance downwelling velocity
 69 and, by association, the component of slab driven flow (Bercovici et al., 2000).

70 The above motivates us to test the degree to which the inclusion of weak plate mar-
 71 gins may alter the general conclusions that: 1) Pressure gradients provide a significant
 72 driving component for asthenosphere flow; 2) Locally, asthenosphere flow can provide
 73 a plate driving force; and 3) Offsets in flow directions between the lithosphere and as-
 74 thenosphere can occur.

75 2 Modeling Methods

76 We used the community finite element code CitcomS to solve the equations for mass,
 77 momentum, and energy conservation in a spherical shell (Zhong et al., 2000; Tan et al.,
 78 2006; Zhong et al., 2008). We assumed mantle convection was driven by both bottom
 79 and internal heating. The bottom heating Rayleigh number and dimensionless internal
 80 heat ratio are set to $1e5$ and 20 respectively. Both are referenced to the viscosity of the
 81 lower mantle. Viscosity was radially stratified to simulate a model lithosphere, model
 82 asthenosphere, and model lower mantle. A high reference viscosity (200) was set for the
 83 model lithosphere to a non-dimensional depth of 0.95 . The asthenosphere reaches to depth
 84 of 0.88 , and was given a power law rheology with a power law exponent of 2 . The lower
 85 mantle was set to reference a viscosity of 1 with a Newtonian rheology.

86 A modified version of CitcomS allows for plate margin formation (Foley & Becker,
 87 2009). When stresses in the model domain exceed a yield stress value, σ_y , viscosity drops.
 88 This simulates plate breaking and weak margin formation without needing to resolve de-
 89 formation along finite faults (Moresi & Solomatov, 1998; Tackley, 1998). We start our
 90 models with a strong lid (high yield stress), then lower the yield stress, using the out-
 91 put of the higher yield stress run as the input for the lower yield stress experiment. Once
 92 the model transitions from single to multiple plate behavior, we ramp up the plate strength
 93 again. We increase the yield stress, beyond the original single-plate value, using the plate-
 94 like behavior model as the initial condition. This provides a test to see if non-Newtonian
 95 viscosity allows for hysteresis effects akin to those that can occur in models with temperature-
 96 dependent viscosity (Weller & Lenardic, 2012; Lenardic et al., 2016).

97 We will show results from a case where the lid did not yield (stagnant lid) with $\sigma_y =$
 98 $3.0 * 10^3$, a case with yield generated plate margins and plate-like behavior (mobile lid)
 99 with $\sigma_y = 2.8 * 10^3$, and additional cases with $\sigma_y = 3.0 * 10^3$, $4.0 * 10^3$, $5.0 * 10^3$ that
 100 maintain mobile lid behavior.

101 All results were taken after statistical steady state was achieved. Statistical steady
 102 state was determined based on Nusselt number and rms velocity time series. Experiments
 103 were run with a numerical resolution of $65 \times 65 \times 65$ nodes per spherical cap (the full spher-
 104 ical domain was spanned by 12 caps).

105 3 Results

106 We visualize isotherms and yielding locations for our model cases in Figure 2. The
 107 results are from models with A) strong plate margins ($\sigma_y = 3 * 10^3$) in a stagnant lid
 108 state B) a stagnant lid start with weaker plate margins ($\sigma_y = 2.8 * 10^3$) C) a mobile
 109 lid start with strong plate margins ($\sigma_y = 3 * 10^3$) and D) a mobile lid start with stronger
 110 plate margins ($\sigma_y = 5 * 10^3$). Yellow regions show where the lithosphere is yielding.
 111 Hot (red) and cold (blue) isotherms are also plotted. Red isotherms map the central re-
 112 gion of mantle upwellings. Blue isotherms map cold sinking lithosphere.

113 The lithosphere, or 'lid', of Case A in Figure 2 is not yielding. This leads to stag-
 114 nant lid mode of convection. The cold isotherm, that is prominent in the other cases,
 115 remains within lithosphere. There are mantle downwellings, but they occur at higher tem-
 116 peratures than the active lid cases (this is consistent with stagnant lid convection be-
 117 ing associated with higher internal mantle temperatures than active lid cases). Multi-

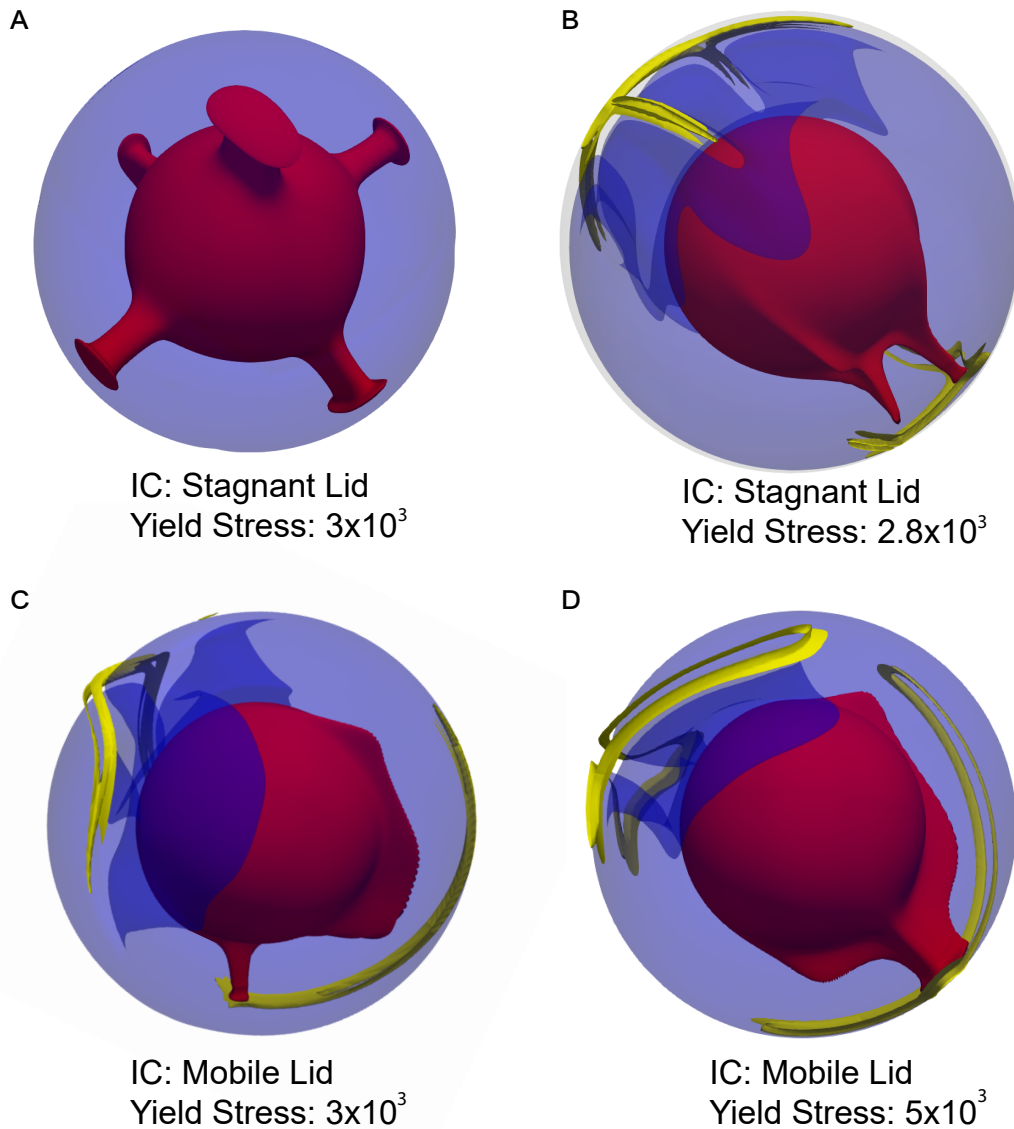


Figure 2. Temperature and yielding visuals from select cases A) initial condition of stagnant lid with a yield stress of 3×10^3 B) initial condition of stagnant lid with a yield stress of 2.8×10^3 , C) initial condition of mobile lid with a yield stress of 3×10^3 , and D) initial condition of mobile lid with a yield stress of 5×10^3 . Colored spheres show isotherms in red (hot) and blue (cold), while yellow regions show where the lithosphere is yielding. Locations where the inner red sphere reach out from the center are upwellings and locations where the blue layer deviates from the outer sphere are downwellings.

118 ple upwellings signify that this case is associated with relatively short convective wave-
119 lengths.

120 Cases B, C, and D are yielding, indicated by the yellow regions above downwellings
121 and upwellings. All three are in a mobile lid mode of convection. Yielding areas are lin-
122 ear features situated over regions of dominantly vertical mantle motion. The blue isotherms

123 indicate that the lithosphere is "subducting" into the mantle. All three cases tend to-
 124 ward degree-1 convection (i.e., long wavelength flow).

125 Figure 3 shows radially averaged horizontal velocity profiles with insets showing
 126 averaged viscosity profiles over asthenosphere depths (note that the velocities are rms
 127 values; velocities change direction, for all the cases, at the asthenosphere-lower mantle
 128 boundary). Profiles are for the cases of A) a strong (black) lid, B) a weak (blue) lid, and
 129 an increasingly strong lid with a mobile initial condition in C) red, D) teal, and E) brown.
 130 Figure 3A reveals an immobile lithosphere. With no lid motion, asthenosphere flow lacks
 131 a plate-driven shear component. It develops a parabolic flow profile, indicative of pressure-
 132 driven flow, and flows faster than the lithosphere and the lower mantle. The weaker lid
 133 and mobile initial condition cases show a fast moving lithosphere, indicating a mobile
 134 lid state. As plate margin strength is increased, the lithosphere slows down (Fig. 3B-
 135 E). In the mobile lid results, average lithosphere velocity exceeds asthenosphere veloc-
 136 ities when lid strength is weaker, but asthenosphere velocities exceed lithosphere veloc-
 137 ities as plate margin strength increases. Overall, velocities are increased everywhere in
 138 the mobile lid cases when compared to the stagnant lid case. Lower mantle flow reverses
 139 direction from upper mantle flow and shows a nearly uniform velocity with depth. Whole
 140 mantle convection is maintained for all cases.

141 Although asthenosphere velocity does not, on average, exceed plate velocity in the
 142 weak margin cases, the global velocity profiles indicate that there is still a component
 143 of pressure driven flow in the asthenosphere. If the asthenosphere responded passively
 144 to plate motion (driven by slab-pull and/or ridge-push), then the velocity profile within
 145 it should take the form of Couette flow (shear driven flow with a linearly decreasing flow
 146 profile). Our model profiles differ from that expectation (Fig. 3B & C). As plate mar-
 147 gin strength is increased, the component of pressure driven flow increases, becoming more
 148 prominent in the flow profiles and leading to asthenosphere velocities exceeding litho-
 149 sphere velocities (Fig. 3E)

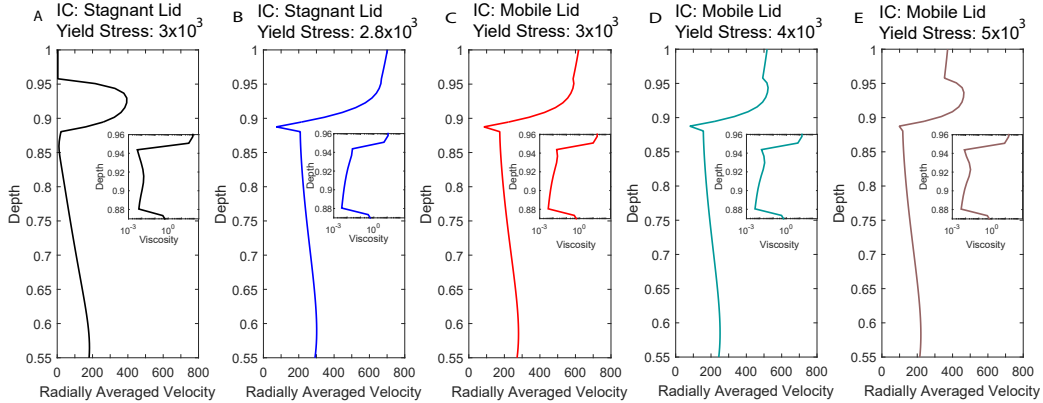


Figure 3. Spherically averaged velocity profiles with inset average viscosity profiles over asthenosphere depths. Profiles are for a A) strong (black) lid, B) weak (blue) lid, and an increasingly strong lid with a mobile initial condition in C) red, D) teal, and E) brown. Velocities are rms values and flow reverses direction from the upper to the lower mantle.

150 The viscosity of the lithosphere decreases below its reference value where stress is
 151 above the designated yield stress. Low viscosity develops dynamically in the asthenosphere
 152 owing to a power law viscosity (Fig. 3inset). Viscosity for the stagnant lid case
 153 displayed two local minima in the asthenosphere with a maximum in its central region.
 154 Weak margin, mobile lid cases had one local minima near the base of the asthenosphere.

As margin strength increased, while maintaining an active lid, a second viscosity minima developed at the lithosphere-asthenosphere boundary (Fig. 3inset). The mobile lid results are associated with cooler interior mantle temperatures than the stagnant lid case and internal temperatures increase with plate margin strength: Average internal mantle temperatures from the cases of Figure 3 are: A) 0.61 B) 0.37 C) 0.39, D) 0.41, E) 0.45.

Local flow profiles can vary from the spherically averaged profiles. Figure 4 presents a view of one such location for two mobile lid cases, A) weak plate margins and B) strong plate margins (from Fig. 2B & D respectively). A perspective view of flow vectors, colored by viscosity, is plotted on the left, with the matching 2D local flow profile on the right. The weak margins case (Fig. 4A) profile was taken near a convergence zone, indicated by the low (yielding) lithosphere viscosity. This profile shows asthenosphere flow (indigo arrows) rotating with depth away from lithosphere direction and to the left (toward the viewer), showing a local region where asthenosphere flow deviates from lithosphere direction with depth. While overall velocities are similar to the global average, the local profile reveals max asthenosphere velocities exceeding lithosphere velocity. This indicates that the ratio of pressure to shear driven flow is larger in this local region than it is on average.

The features discussed above become more pronounced when plate margin strength is increased, while mobile lid convection is maintained. Figure 4B shows asthenosphere flow direction (indigo arrows) offset to the right of lithosphere direction, rotating away from the viewer. In this case, the flow direction offset is prominent throughout all of the asthenosphere, and this offset is also sustained farther away from the convergence zone than in the weakest lid case (Fig. 4A).

4 Discussion

Inclusion of plate-like behavior does not qualitatively alter the principal conclusions of Semple and Lenardic (2018). Quantitatively, the globally averaged profiles of plate-like models show a milder component of pressure-driven asthenosphere flow relative to models that do not allow for weak plate margins. Globally, for weak margins, asthenosphere flow velocities may not exceed plate velocities, but they can do so locally. Within those regions, asthenosphere flow can become offset, with depth, from the direction of lithosphere motion (Fig 4).

In addition to the above, we find a dependence of global plate driving forces on the strength of plate margins (Fig. 3). A stagnant-lid mode results in a large component of pressure driven flow in the asthenosphere. Weak plate margin, mobile-lid behavior leads to a larger component of slab-pull driven flow in combination with a milder component of asthenosphere-drive (Höink et al., 2011). As plate margin strength increases, the component of asthenosphere-drive relative to slab-pull increases. This supports the possibility that plates can be driven by both slab-pull and asthenosphere-drive forces (Höink & Lenardic, 2010; Höink et al., 2011; Coltice et al., 2019).

Our results reveal a hysteresis effect on the value of plate margin strength that allows for mobile-lid convection. This allows different modes to exist under equivalent parameter conditions (2). The potential of hysteresis and bistable tectonics is not a new observations in coupled convection and tectonics models (Weller & Lenardic, 2012). However, those previous models relied on the interaction of temperature-dependent mantle viscosity and dynamic plate margin formation. Our models show that a non-Newtonian upper mantle rheology, together with plate margin formation, also allows for bistability. Future models that combine the effects should be considered in order to fully map the range of parameter space that allows for tectonic bistability.

As well as more fully mapping hysteresis effects, there are other expansions to be considered for our experiments. Our power law rheology exponent is below the preferred

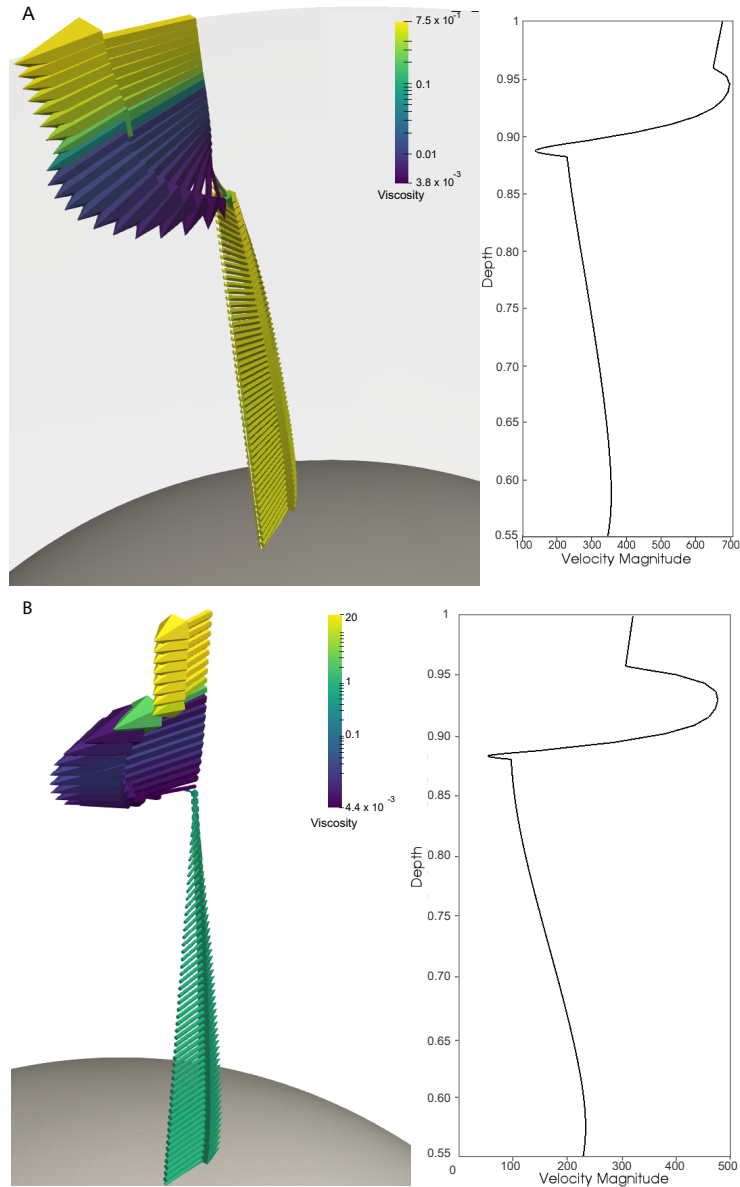


Figure 4. Local velocity profiles for for cases A) $\sigma_y = 2.8 * 10^3$. and B) $\sigma_y = 5 * 10^3$. Left: Perspective view on local profile results where colors indicate viscosity. Right: 2D velocity profile from the matching left image. indigo arrows show asthenosphere depths where asthenosphere flow in both cases rotates away from lithosphere flow and locally leads plate velocities.

205 rock-like value ($n = 3$) that Semple and Lendardic (2018) tested (Hirth & Kohlstedt,
 206 2013). We kept a lower power law exponent in the interest of keeping the computational
 207 burden lower. With non-Newtonian rheology, and yield stress conditions, resolution and
 208 run time requirements become large. This is not insurmountable and a sub-goal of our
 209 preliminary results was to show that the challenge is worth undertaking (had our new
 210 models not confirmed our previous results the motivation to expand them further would
 211 be weaker).

212 5 Conclusions

213 Allowing for a combination of non-Newtonian asthenosphere rheology and plate-
 214 like behavior increases the ratio of slab-pull to asthenosphere-drive forces compared to
 215 models that lack weak plate margins (Sempé & Lendaric, 2018). None the less, con-
 216 vective flow in the upper mantle remains driven by a combination of slab-pull and pressure-
 217 driven flow. In addition, local regions can still exist where 1) asthenosphere velocity ex-
 218 ceeds that of the lithosphere above and 2) asthenosphere flow rotates with depth, be-
 219 coming offset from plate motion.

220 Acknowledgments

221 We'd like to our anonymous reviewers for their comments. All input files necessary to
 222 run our models and generate this data in CitcomS 3.2 can be found on the online repos-
 223 itory, Zenodo, at <https://zenodo.org/record/3922867>.

224 References

- 225 Bercovici, D., Ricard, Y., & Richards, M. A. (2000). The relation between man-
 226 tle dynamics and plate tectonics: A primer. *Geophysical Monograph-American*
 227 *Geophysical Union*, *121*, 5-46. doi: 10.1029/GM121p0005
- 228 Coltice, N., Husson, L., Faccenna, C., & Arnould, M. (2019). What drives tectonic
 229 plates? *Science Advances*, *5*(10). doi: 10.1126/sciadv.aax4295
- 230 Cox, A. (1972). *Plate tectonics and geomagnetic reversals*. W. H. Freeman and Co.
- 231 Foley, B. J., & Becker, T. W. (2009). Generation of plate-like behavior and mantle
 232 heterogeneity from a spherical, viscoplastic convection model. *Geochemistry,*
 233 *Geophysics, Geosystems*, *10*(8). doi: 10.1029/2009GC002378
- 234 Forsyth, D., & Uyeda, S. (1975). On the relative importance of the driving forces of
 235 plate motion. *Geophysical Journal of the Royal Astronomical Society*, *43*, 163-
 236 200. doi: 10.1111/j.1365-246X.1975.tb00631.x
- 237 Hirth, G., & Kohlstedt, D. (2013). Rheology of the upper mantle and the man-
 238 tle wedge: A view from the experimentalists. In *Inside the subduction fac-*
 239 *tory* (p. 83-105). American Geophysical Union (AGU). Retrieved from
 240 <https://agupubs.onlinelibrary.wiley.com/doi/abs/10.1029/138GM06>
 241 doi: 10.1029/138GM06
- 242 Höink, T., Jellinek, A. M., & Lenardic, A. (2011). Asthenosphere drive: A
 243 wavelength-dependent plate-driving force from viscous coupling at the
 244 lithosphere-asthenosphere boundary. *Geochemistry, Geophysics, Geosystems*,
 245 *12*. doi: 10.1029/2011GC003698
- 246 Höink, T., & Lenardic, A. (2010). Long wavelength convection, poiseuille-
 247 couette flow in the low-viscosity asthenosphere and the strength of plate
 248 margins. *Geophysical Journal International*, *180*, 23-33. doi: 10.1111/
 249 j.1365-246X.2009.04404.x
- 250 Lenardic, A., Crowley, J., Jellinek, A., & Weller, M. (2016). The solar sys-
 251 tem of forking paths: Bifurcations in planetary evolution and the search
 252 for life-bearing planets in our galaxy. *Astrobiology*, *16*(7), 551-559. doi:
 253 10.1089/ast.2015.1378
- 254 Lin, P. Y. P., Gaherty, J. B., Jin, G., Collins, J. A., Lizarralde, D., Evans, R. L., &
 255 Hirth, G. (2016). High-resolution seismic constraints on flow dynamics in the
 256 oceanic asthenosphere. *Nature*, *535*, 538-541. doi: 10.1038/nature18012
- 257 Moresi, L. N., & Solomatov, V. S. (1998). Mantle convection with a brit-
 258 tle lithosphere: thoughts on the global tectonic styles of the earth and
 259 venus. *Geophysical Journal International*, *133*(3), 669-682. doi: 10.1046/
 260 j.1365-246X.1998.00521.x
- 261 Schubert, G., Turcotte, D., & Olson, P. (2001). *Mantle convection in the earth and*
 262 *planets*. Cambridge Univ. Press, Cambridge, U. K.

- 263 Semple, A. G., & Lendaric, A. (2018). Plug flow in the earth's asthenosphere.
264 *Earth and Planetary Science Letters*, *496*, 29-36. doi: 10.1016/j.epsl.2018.05
265 .030
- 266 Tackley, P. J. (1998). Self-consistent generation of tectonic plates in three-
267 dimensional mantle convection. *Earth and Planetary Science Letters*, *157(1)*,
268 9-22. doi: 10.1016/S0012-821X(98)00029-6
- 269 Tan, E., Choi, E., Thoutireddy, P., Gurnis, M., & Aivazis, M. (2006). Geoframe-
270 work: Coupling multiple models of mantle convection within a computa-
271 tional framework. *Geochemistry, Geophysics, Geosystems*, *7*, Q06001. doi:
272 10.1029/2005GC001155
- 273 Turcotte, D. L., & Schubert, G. (2014). *Geodynamics*. Cambridge Univ. Press, Cam-
274 bridge, U. K.
- 275 Weller, M. B., & Lenardic, A. (2012). Hysteresis in mantle convection: Plate
276 tectonics systems. *Geophysical Research Letters*, *39(10)*. doi: 10.1029/
277 2012GL051232
- 278 Zhong, S., McNamara, A., Tan, E., Moresi, L., & Gurnis, M. (2008). A bench-
279 mark study on mantle convection in a 3-d spherical shell using citcoms. *Geo-*
280 *chemistry, Geophysics, Geosystems*, *9*, Q10017. doi: 10.1029/2008GC002048
- 281 Zhong, S., Zuber, M. T., Moresi, L., & Gurnis, M. (2000). Role of temperature-
282 dependent viscosity and surface plates in spherical shell models of mantle
283 convection. *Journal of Geophysical Research*, *105(B5)*, 11063-11082. doi:
284 10.1029/2000JB900003